

The four vectors $\mathbf{a}_1, \mathbf{a}_2, \mathbf{a}_3, \mathbf{a}_4$ are of size N , the same as the vector \mathbf{I} . They can be horizontally concatenated to form the matrix, $\mathbf{A} = (\mathbf{a}_1, \mathbf{a}_2, \mathbf{a}_3, \mathbf{a}_4)$ of size $N \times M$, where $M = 4$ is the number of scaling factors in Eq. (9). Then, Eq. (9) can be written as

$$\mathbf{Y} = \mathbf{I} - \mathbf{I}_o = \mathbf{A}\mathbf{f}; \quad \text{with} \quad \mathbf{f} = (f_{CO_2}, f_T, f_Q, f_{T_s})^T \quad (10)$$

In Eq. (10) we have $M = 4$ unknowns and $N = 227$ observations, therefore we can use Least Squares to seek for an optimal solution. We have checked that no further constraints have to be considered to get an estimate $\hat{\mathbf{f}}$ of \mathbf{f} and its covariance matrix, $\mathbf{S}_{\hat{\mathbf{f}}}$, therefore we can use *unconstrained* Least Square, this is important because it means that the final solution is not biased,

$$\hat{\mathbf{f}} = (\mathbf{A}^T \mathbf{S}_I^{-1} \mathbf{A})^{-1} \mathbf{A}^T \mathbf{S}_I^{-1} \mathbf{Y}; \quad \text{and} \quad \mathbf{S}_{\hat{\mathbf{f}}} = (\mathbf{A}^T \mathbf{S}_I^{-1} \mathbf{A})^{-1} \quad (11)$$

where \mathbf{S}_I is the observational covariance matrix of the interferometric radiances. The observational covariance matrix, \mathbf{S}_I has been constructed by considering that for the IASI spectrum, \mathbf{S}_R , which, in turn, is constructed on the basis of IASI radiometric noise. \mathbf{S}_R is non-diagonal because the IASI spectrum is apodised. The transformation of \mathbf{S}_R to \mathbf{S}_I has been performed taking correctly into account the apodisation effect.

Finally, an estimate \bar{q}_{CO_2} of the total column amount of CO_2 is obtained by

$$\bar{q}_{CO_2} = (1 + \hat{f}_{CO_2}) \int_{p_g}^0 q_{CO_2}(p) dp = (1 + \hat{f}_{CO_2}) \bar{q}_{CO_2,o} \quad (12)$$

where p_g is the ground pressure and with $\bar{q}_{CO_2,o}$ the total column amount of the CO_2 reference profile. The accuracy, e_{CO_2} of the estimate is given by

$$e_{CO_2} = \sqrt{S_{\hat{\mathbf{f}}}(1, 1)} \bar{q}_{CO_2,o} \quad (13)$$

We should observe that in the retrieval procedure we also need a reference mixing ratio profile of CO_2 for the retrieval algorithm. Using the same approach as that shown in [3], we have checked that the choice of either an uniform CO_2 profile (constant mixing ratio with the altitude) or a non-uniform profile is not critical. This sensitivity check has been performed by considering retrievals obtained with uniform profiles with a fixed mixing ratio value of 385 ppmv (see Fig. 3) and non-uniform CO_2 profiles obtained from ECMWF analysis (e.g., see Fig. 2 in ref [3]) collocated in time and space with the JAIVEx soundings. As a result we have a difference, (non-uniform)-(uniform), which does not exceed +1 ppmv.

The various scaling factors which are determined within the retrieval scheme also provide a good quality check of the final solution. We do not expect dramatic variations in the values corresponding to T_s , T and H_2O . The reference atmospheric parameters have been obtained by a physical inversion of the same spectra we use to retrieve CO_2 . In case we find large variations, it is likely that the retrieval has failed due to some unknown source of additional error, most likely cloudiness. For temperature we expect at most to have variations below ± 1 K, for water vapour we could expect some larger deviation from the reference, because the IASI retrieval may have a large uncertainty in the lower troposphere. However, variation larger than 20% are suspicious and the retrieval is flagged as of poor quality in this case.

To demonstrate the PSI methodology, we have applied it to a set of 22 clear sky, sea surface IASI soundings which were recorded during the 2007 JAIVEx experiment [38], which took place in the Gulf of Mexico. This set of IASI spectra has been already used to check the PSI retrieval for CO_2 by [3], which the reader is referred to for further details. Six of this spectra are nadir view spectra, whereas the remaining 16 correspond to an angle of $\approx 22.5^\circ$. Furthermore, the spectra have been recorded on different days. Six (those at nadir) on 29 April 2007, sixteen

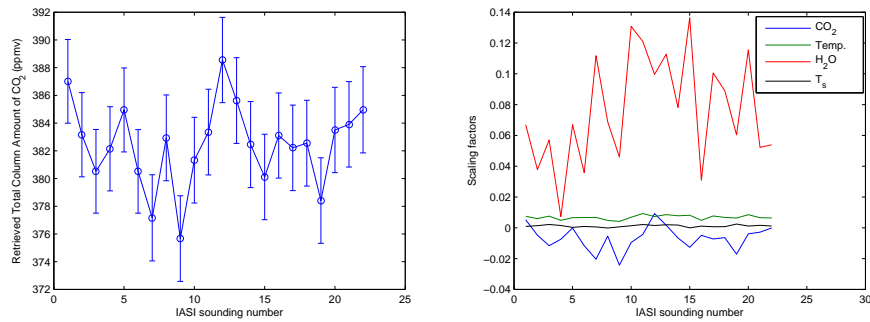


Fig. 4. (left) Retrieved CO_2 for the JAIVEx experiment; (right) retrieved scaling factors for the JAIVEx experiment.

on 30 April 2007. For that period the global average value for CO_2 was 384.10 ppmv, according to the NASA Earth System Monitoring Laboratory (Global Monitoring Division) [39]. For the JAIVEx experiment, the reference atmospheric state, consisting of (T_s, T, Q, O) was retrieved by initializing the physical scheme with a first guess obtained by EOF regression. From a comparison with in situ dropsonde observations, we know that the final results for H_2O were determined with an accuracy not better than 15%. In contrast, the accuracy for T_s was within ± 0.5 K and that for the temperature profile was within ± 1 K in layers of 1 km width in the lower troposphere [32]. Figure 4 shows the retrieved values of \bar{q}_{CO_2} corresponding to the 22 IASI soundings. It is seen that the accuracy, computed through Eq. (13) of the estimate is ± 3 ppmv (that is better than 1%) at the level of the single IASI IFOV, hence at a spatial resolution of 12 km. The average of the retrieval for 29 April 2007 is (383.0 ± 1.2) ppmv, whereas that for 30 April 2007 is (382.2 ± 0.8) ppmv to be compared to the global average value of 384.10 ppmv for that period. It is important to note that if we consider the standard deviation of the retrieval shown in Fig. 4 we get the value of ± 3 ppmv, which is equal to the accuracy of each single observation. In other words, the variability we see in Fig. 4 is that of the random error of the IASI observations and is not due to an additional unknown source of random noise or bias. To further check the quality of the retrieval it is also interesting to look at the behaviour of the four scaling factors. These are shown in Fig. 4. It is seen that the effect of T_s and T is marginal. The scale factor for the skin temperature is almost zero, which attests to the accuracy of the reference value used for T_s in our scheme. The scaling for the temperature profile is in any case below 1%, which again is a sign of the quality of the reference we used for the retrieval. Conversely, as expected, the effect of H_2O is more conspicuous and the related scaling factor can attain variations as large as 14%.

Finally, the problem of the interdependence between the total column amount of CO_2 and the temperature profile is addressed. First, we note that through the scaling factor, f_T we retrieve a bulk temperature of the atmosphere and not a detailed temperature profile. The fact that we have independent information for both f_T and f_{CO_2} is evidenced by the existence of the *unconstrained* Least Squares solution we get through Eq. (11). A strong interdependency between the two parameters f_T and f_{CO_2} would yield a Kernel **A** highly ill-conditioned. However, normally the conditioning number of this Kernel is below 100, which means that the linear system expressed by Eq. (10) is made up with equations, which are largely independent. The interdependency between atmospheric parameters can be also analysed by looking at the a-posteriori

covariance matrix, \mathbf{S}_f or better at the correlation matrix, \mathbf{C}_f defined according to

$$C_f(i, j) = \frac{S_f(i, j)}{\sqrt{S_f(i, i)S_f(j, j)}} \quad i, j = 1, \dots, M = 4 \quad (14)$$

Keeping in mind the definition of the \mathbf{f} -vector in Eq. (10), a typical example of the correlation matrix \mathbf{C}_f is shown in Eq. (15) below

$$\mathbf{C}_f = \begin{pmatrix} 1.000, & -0.14, & 0.130, & -0.49 \\ -0.14, & 1.000, & 0.850, & 0.540 \\ 0.130, & 0.850, & 1.000, & 0.260 \\ -0.49, & 0.540, & 0.260, & 1.000 \end{pmatrix} \quad (15)$$

From the first row of this matrix we learn that the correlation of the CO₂ total column amount with temperature and water vapour is very poor: the correlation is -0.14 with temperature and 0.13 with water vapour. Furthermore, these two correlations have opposite sign and tend to cancel out. In contrast, the correlation with surface temperature reaches the value of -0.5. This result says that for the retrieval of the total column amount of CO₂ a good reference value of the surface temperature is much more critical than a good reference value for temperature and water vapour profiles. Also from Eq. (15), second row, we note a relatively high interdependency between T and Q , and T and T_s .

In summary, for the retrieval scheme we have developed the interdependence between temperature profile and the total column amount of CO₂ is not a major concern, a source of possible bias is much more linked to T_s , for which we need a good reference value to initialize the inverse scheme to retrieve \bar{q}_{CO_2} .

3.2. The case of CO, N₂O and CH₄

The retrieval methodology developed for CO₂ has been also applied to CO, N₂O and CH₄. Of course, the partial interferogram depends on the given gas and is selected in order to minimize interfering effects from other species.

For the case of CO, a linear molecule, its spectrum (at the IASI spectral resolution) has regularly spaced spectral lines in the atmospheric window between 2080 and 2200 cm⁻¹. The line spacing is ≈ 2 cm⁻¹ in the spectral domain, which yields a resonance in the interferogram space at the inverse of two times the line spacing, that is 0.25 cm. The partial interferogram we use for CO total column amount retrieval is obtained by Fourier transforming the IASI band 3 alone. The interferogram interval extends from 0.2230 to 0.3118 cm and is shown in Fig. 5(a) for the case of a tropical model of atmosphere. At the IASI sampling interval, we have a total of $N = 136$ data points. In this range, apart from the ubiquitous presence of water vapour, CO is the most important contributors to the spectrum, with N₂O and O₃ playing a secondary role.

N₂O is a linear molecule as well, with regularly spaced absorption lines at the spectral IASI resolution. The main N₂O absorption bands (ν_1 and ν_3 absorptions bands) are located in IASI band 1, 2 and 3. For this reason, to take advantage of the contribution from all lines, the interferogram from N₂O is obtained by Fourier transforming the whole IASI spectrum (band 1, 2 and 3). The partial interferogram for N₂O is shown in Fig. 5(b) and extends over two separate intervals from 1.0459 to 1.0499 cm and 1.1220 to 1.1270 cm, respectively, for a total of 40 data points. N₂O is the most difficult gas to retrieve. Its ν_1 -absorption band overlaps that of methane at 1306.6 cm⁻¹, and the ν_3 in the short-wave region overlaps that of CO₂. The partial interferogram range we have selected is the only short portion of the whole interferogram where the main contributor is N₂O, whereas the contribution from interfering species, especially by CH₄ is minimized.

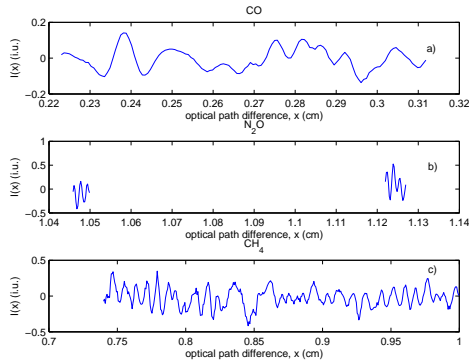


Fig. 5. Partial interferogram used for a) CO, b) N₂O and c) CH₄. (1 i.u.= 1 W m⁻²sr⁻¹).

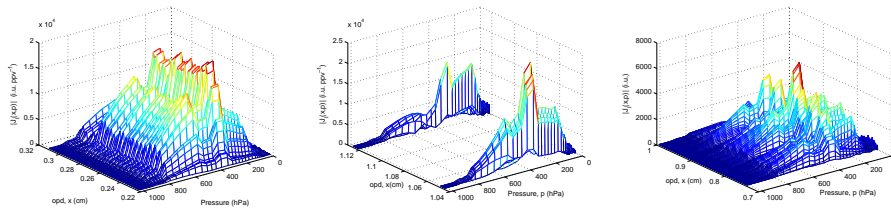


Fig. 6. Jacobian derivative of $I(x)$ with respect to the volume mixing ratio of CO (left); N₂O (middle); CH₄ (right) (1 i.u.= 1 W m⁻²sr⁻¹).

Finally, CH₄ is present in the IASI band 2 (ν_4 absorption band centred at 1306.2 cm⁻¹). Methane is not a linear molecule, however its spectrum also generates (at IASI spectral resolution) a characteristic wave-like structure in the interferogram domain. For the purpose of the retrieval of the total column amount of CH₄, the interferogram has been obtained by considering only the IASI band 2, which limits potential interfering effects mostly to N₂O alone. The partial interferogram we have selected for the retrieval of CH₄ is shown in Fig 5(c). It extends from 0.7399 to 1 cm for a total of 412 data points. In this range the contribution from N₂O is nearly zero.

The reference profiles we use for CO, CH₄, N₂O and CO₂ as well are summarized in Fig. 3. The total column amount from the reference profile yields 109 ppbv for CO, 306 ppbv for N₂O and 1646 ppbv for CH₄.

As for CO₂ we have that the sensitivity of our retrieval methodology extends to a large portion of the troposphere. Normally, the lower troposphere, which extends from 1000 to \approx 800 hPa shows a very poor sensitivity, mostly for CH₄ and N₂O, as it is possible to see from Fig. 6, which shows mesh surfaces of the Jacobian derivative of the interferogram radiance with respect to the volume mixing ratio of CO, N₂O and CH₄, respectively.

For the set of 22 IASI spectra from the JAIVEx experiment, Fig. 7 shows the retrieval for the total amount of CO, N₂O and CH₄, respectively. The accuracy of the retrieval for a single IASI observations is $\approx \pm 1.5$ ppbv, $\approx \pm 13$ ppbv and $\approx \pm 0.015$ ppmv respectively for CO, N₂O and CH₄. Figure 7 shows that the retrieval is largely in agreement with the global annual cycle of CO, CH₄ and N₂O, respectively (e.g., [40]). In addition, as already found for the case of CO₂, we also have that the standard deviation of the retrieved values for CH₄ and N₂O perfectly

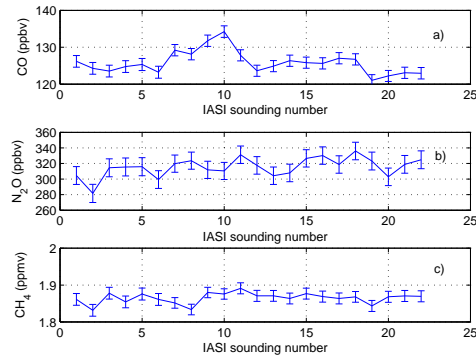


Fig. 7. Retrieval analysis for the JAIVEx experiment. a) CO; b) N₂O; c) CH₄.

parallels the accuracy assessed through the retrieval covariance matrix, Eq. (11), that is ± 15 ppbv for CH₄ and 13 ppbv for N₂O. For CO the standard deviation is 3 ppbv, which is about two times the accuracy. This is quite compatible with the high variability of this atmospheric gas.

4. Application to IASI for the Mediterranean sea

To check the quality and reliability of the retrieval algorithm for trace gases when applied to a large set of IASI data, we have focused on the Mediterranean basin for the period of July 2010. We have a total of 34719 IASI soundings, which have been checked for clear sky using the IASI stand alone cloud detection scheme described in [28–31]. Each IASI sounding has been inverted for T_s and T, Q, O . These parameters have been used as the reference state in the sequential retrieval for trace gases.

The maps for the four trace gases considered in this study are shown in Fig. 8. The original IASI retrieval has been smoothed with a Wiener filter [41] and projected on 0.5×0.5 deg (lat \times lon) grid. To a variable degree, all maps show a positive gradient into the direction North-West to South-East. This is in agreement with the general circulation over the Mediterranean sea for the month of July. For the case of CO₂ we have that the total column amount is distributed over a range of values from 380 to 390 ppmv, with an average of 384.8 ppmv. This can be compared to the global average value of the annual cycle for the month of July 2010, which according to the NASA Earth System Monitoring Laboratory (Global Monitoring Division) [39] is equal to 387.21 ppmv.

The average values for CH₄, N₂O, and CO are 1926 ppbv, 313 ppbv and 88 ppbv, respectively. The value observed for CH₄ is a bit higher of that credited to this gas from ground based observations at mid-latitude, that is 1874 ppbv [40], whereas for N₂O our average concentration of 313 ppbv is slightly smaller than the global value, which is 324 ppbv [40]. These differences have to be expected when we compare sea surface measurements with satellite observations, which are not sensitive to the planetary boundary layer (e.g. see Fig. 6). The observed differences just says that the volume mixing ratio of both N₂O and CH₄ is not uniform with the altitude. For N₂O aircraft observations tend to confirm that the concentration of N₂O in the boundary layer is some 10-15 ppbv larger than that in the open troposphere [42].

For the case of CO, we have to say that this is a gas which has a large time and space variability, so that the comparison with sea surface values makes less sense. What we can say

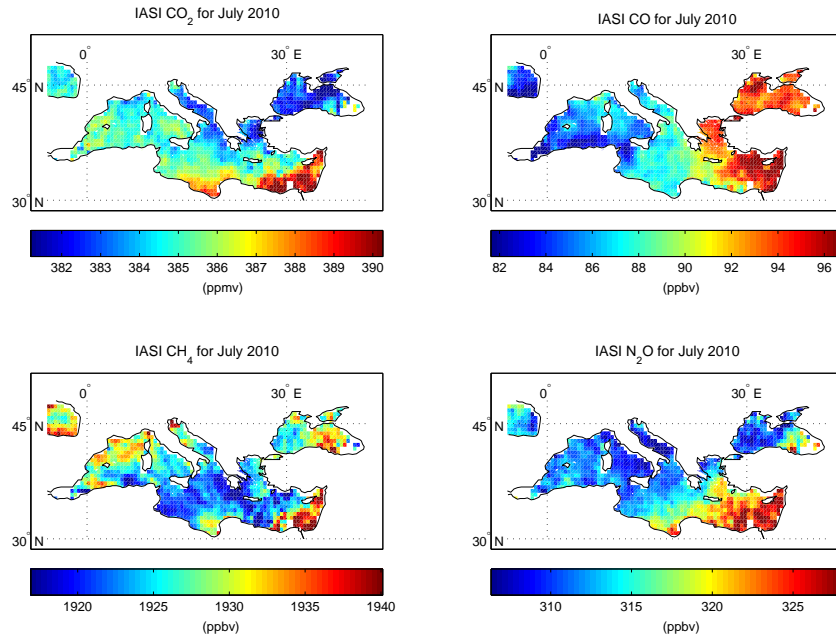


Fig. 8. July 2010 maps derived from IASI soundings. From top left, clockwise, total column amount of CO₂, CO, CH₄ and N₂O, respectively.

is that sea surface observations also show a pronounced annual cycle with its minimum in the summer season. Also, aircraft records show that the summer vertical spatial distribution of CO concentration has a rapid decrease from the boundary layer to the free troposphere [43]. This behaviour is in agreement with our retrieval. We also stress that our CO retrieval results are in excellent agreement with those obtained with the LATMOS-ULB algorithm [23, 24]. The comparison to our CO retrievals is shown in Fig. 9. The LATMOS-ULB mean value for the month of July is 89.4 ppbv with a variability of 9.08 ppbv over the basin. This figure can be compared to our figure of 88.2 ppbv for the mean and 7.20 ppbv for the variability. The slightly lower mean and variability obtained using our retrieval is likely to be a result of the use of a more stringent cloud mask in the processing of the IASI data. Nevertheless, the two maps plotted in Fig. 9 show remarkably consistent features and display the same horizontal spatial gradients.

For the CO₂ case we have carried out a comparison with AIRS CO₂ level 2 products by projecting IASI and AIRS CO₂ fields on the same 2 × 2 deg (lat × lon) grid. Results are shown in the maps plotted in Fig. 10. It is evident that the results shown in the AIRS map display all the elements of a random behaviour. Furthermore, the AIRS CO₂ level 2 data give an average value of 391.5 ppmv with a variability (standard deviation) of 2.8 ppmv. This means that, even taking into account its variability, the AIRS estimate of the average value exceeds both the value of the annual cycle for the month of July (387.21 ppmv) and the annual trend for 2010 (388.58 ppmv [39]). In contrast, our scheme retrieves an average value of 384.8 ppmv, which, within a variability of 4.8 ppmv, is in agreement with both the cycle and the trend. Besides, this variability of 4.8 ppmv is not just random. It reflects a North-to-South gradient as shown in Fig. 10. This pattern is absent in the AIRS results which clearly show that the variability of the retrieval is fundamentally random.

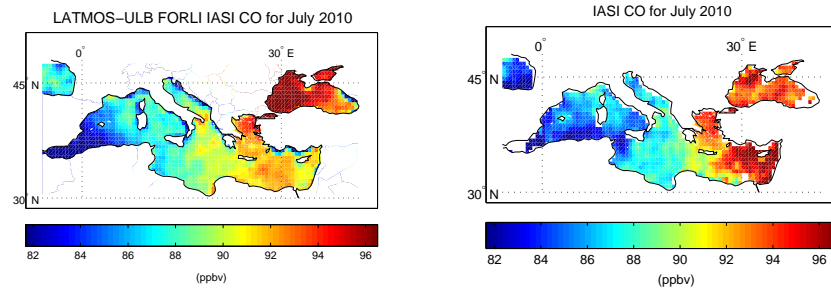


Fig. 9. July 2010 maps derived from IASI soundings. LATMOS-ULB retrieval scheme (left); this study (right).

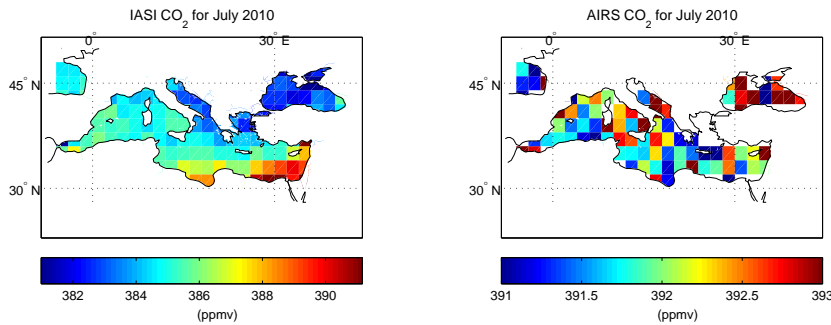


Fig. 10. CO₂ monthly map on 2 × 2 deg grid. Left, IASI. Right, AIRS.

As shown in Fig. 10, the North-to-South gradient retrieved by the IASI PSI scheme is in agreement with the observations of CO₂ and CH₄ at the sea surface level obtained from the GAW WMO network for the month of July 2010. For the case of CO₂ it is interesting to see that the IASI PSI retrieval is capable of capturing the local minimum around Filokalia station (see Fig. 11). The capability of the PSI methodology of capturing the correct horizontal gradients is also evident in the case of methane. These results support our claim of being able to retrieve the concentration of trace gases to an unprecedented accuracy. Also, we note that the North-West to South-East gradient for CO₂ and CH₄ is in agreement with the known biogenic activity of the Mediterranean sea. In summer the North-West part of the sea is a sink for CO₂, whereas the South-East part behaves like a source [44].

5. Conclusion

We have demonstrated that the technique of partial correlation interferometry applied to IASI observations is capable of improving the accuracy of trace gas retrieval to the unprecedented values of ± 3 ppmv for CO₂, ± 13 ppbv for N₂O, ± 1.5 ppbv for CO and, finally ± 15 ppbv for CH₄ for each single IASI observation with a horizontal spatial resolution of ≈ 12 km. The analysis of IASI data over the relatively small basin of the Mediterranean sea has shown that we can retrieve relatively small scale structures. This has allowed us to detect for the first time a summer North-West to South-East gradient in the concentration of trace gases of climatological importance. The pattern of CO₂ is consistent with the known biogenic activity of the Mediterranean sea in July. The global monthly maps of methane, carbon monoxide, carbon

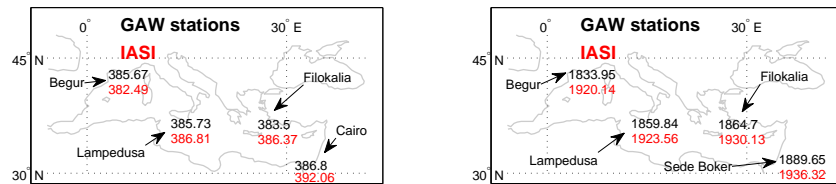


Fig. 11. Comparison of IASI retrieval with observations at sea surface stations. CO₂ (left); CH₄ (right).

dioxide and nitrous oxide retrieved using IASI data are consistent with the known annual cycles of these trace gases. As an example, we were able to detect the strong decrease of carbon monoxide concentration in July, when the concentration of this gas in the open troposphere goes below 100 ppbv. It has also to be stressed that our scheme is a physical-based algorithm, which exploits the capability of the σ -IASI forward model to compute analytical Jacobian derivatives. Examples of analytical Jacobian have been provided that show the sensitivity of IASI to the vertical concentration of trace gases. Because of this capability, our scheme can be easily generalized to retrieve also information along the vertical. However, the important aspect of the present methodology is that it is based on unconstrained Least Square, which yields unbiased results. If we want to move to the retrieval of vertical profiles, we will need additional constraints, which inevitably will add bias to the final solution. To conclude, the vertical spatial resolution and the magnitude of the bias will depend on the background constraint, an effect which will be investigated in future work.

Acknowledgments

IASI has been developed and built under the responsibility of the Centre National d'Etudes Spatiales (CNES, France). It is flown onboard the Metop satellites as part of the EUMETSAT Polar System. The IASIL1 data are received through the EUMETCast near real time data distribution service. We thank Dr Stuart Newman (Met Office) for providing the JAIVEx data. The ground based measurements in Lampedusa and Sede Boker have been provided by NOAA/ESRL and have been downloaded from (<http://www.esrl.noaa.gov/gmd/dv/iadv/>). The ground based measurements in Begur and Finokalia have been provided by Laboratoire des Sciences du Climat et de l'Environnement (<http://www.lscse.ipsl.fr/>). The ground based measurements in Cairo have been provided by the Egyptian Meteorological Authority (<http://ema.gov.eg/>). The ground based measurements in Lampedusa for what concerns N₂O have been provided by the Italian Agency ENEA. Work supported by project Ritmare-Ricerca Italiana per il Mare (CNR-MIUR)